A host dicer is required for defective viral RNA production and recombinant virus vector RNA instability for a positive sense RNA virus

Xuemin Zhang and Donald L. Nuss*

Center for Biosystems Research, University of Maryland Biotechnology Institute, Shady Grove Campus, Rockville, MD 20850

Edited by Reed B. Wickner, National Institutes of Health, Bethesda, MD, and approved August 29, 2008 (received for review July 25, 2008)

Defective interfering (DI) RNAs, helper virus-dependent deletion mutant RNAs derived from the parental viral genomic RNA during replication, have been described for most RNA virus taxonomic groups. We now report that DI RNA production in the chestnut blight fungus, *Cryphonectria parasitica*, persistently infected by virulence-attenuating positive sense RNA hypoviruses, depends on one of two host dicer genes, *dcl-2*. We further report that nonviral sequences that are rapidly deleted from recombinant hypovirus RNA virus vectors in wild-type and dicer gene *dcl-1* deletion mutant strains are stably maintained and expressed in the Δ*dcl-2* mutant strain. These results establish a requirement for *dcl-2*, the *C. parasitica* dicer gene responsible for antiviral defense and generation of virus-derived small interfering RNAs, in DI RNA production and recombinant virus vector RNA instability.

defective interfering RNA | hypovirus | RNA silencing | RNA recombination

Virus RNA recombination is an important component of virus evolution that contributes to the emergence of new viruses (reviewed in 1) and the generation of internally deleted mutant RNAs, termed defective interfering (DI) RNAs, that are derived from, and are dependent on, the parental viral genomic RNA (2). The presence of DI RNAs can suppress parental virus RNA accumulation, leading to attenuation of symptoms (3) and persistent virus infections (4, 5). Rapid recombination also appears to be an underlying cause of the instability and deletion of foreign, nonviral sequences from recombinant viral RNA vectors (6; reviewed in 7). Genome instability presents one of the most important obstacles to the use of recombinant RNA viruses as gene expression vectors for various practical applications, including gene therapy (8–10).

Single-strand, positive sense mycoviruses in the family *Hypoviridae*, hypoviruses that persistently infect and attenuate virulence of the chestnut blight fungus, *Cryphonectria parastica*, generate internally deleted DI RNAs at a very high frequency (11, 12). Efforts to use recombinant hypoviruses to express foreign genes also have encountered the limitation of instable nonviral nucleotide sequences (13).

We recently reported that disruption of one of two *C. parasitica* dicer genes, *dcl-2*, results in increased susceptibility to mycovirus infection (14). We subsequently showed that *dcl-2* functions to process mycovirus RNAs into virus-derived small interfering RNAs (vsRNAs) as part of an inducible RNA silencing antiviral response (15). Cloning and characterization of vsRNAs generated from hypovirus CHV1-EP713 revealed a nonrandom distribution of vsRNAs along the 12.7-kb genome RNA. Conspicuous was the very low representation of vsRNA mapping to an internal portion of the 12.7-kb genome RNA that encodes the viral polymerase and helicase domains, from map position 7500 to 11000 (15). It has been postulated that the propensity of hypoviruses to generate internally deleted DI RNAs results in a lower level of substrate for vsRNA biogenesis from this region (15). Here we confirm that the region extending from map position 7348 to 11267 is absent in the DI RNA population. We also report that hypovirus DI RNAs are not produced in *C. parasitica dcl-2* deletion mutant strains. Moreover, nonviral sequences in recombinant hypovirus viral vector RNA, which are rapidly deleted in wild-type and dicer-1 (*dcl-1*) mutant *C. parasitica* strains, are stably maintained in the absence of *dcl-2*. These results establish a role for a host dicer gene in DI RNA production and virus vector RNA instability for a single-strand, positive sense RNA virus.

Results

Hypovirus DI RNA Structure Correlates with Nonrandom Distribution of vsRNAs. Our recent analysis of cloned vsRNAs derived from the 12,712-nt hypovirus CHV1-EP713 RNA in persistently infected *C. parastica* (15) revealed a nonrandom distribution along the viral genome, with very few cloned vsRNAs, all of positive polarity, originating from the region of the genomic RNA spanning map coordinates 7500 to 11000. We predicted that the reduction in full-length viral RNA accumulation because of competition with DI RNAs (Fig. 1*A*) decreased the level of substrate for vsRNA biogenesis from the regions deleted in the DI RNA. This prediction was based on our previous report that the 8- to 10-kb DI RNA species associated with CHV1-EP713 infection retained ≈3.5 kb of each terminus and thus would lack all or portions of the regions of the viral genomic RNA that were underrepresented in the cloned vsRNA population (11). Extensive polymerase chain reaction (PCR) amplification and nucleotide sequence analysis was used to further define the structure of CHV1-EP713–associated DI RNA species.

Hypoviruses do not encode a capsid protein and thus do not form discrete virus particles. Consequently, the accumulation of viral double-stranded (ds) RNA, including dsRNA forms of DI RNAs, is assessed to monitor the extent of virus infection. DI RNAs generally are not observed in the dsRNA fraction isolated from wild-type *C. parasitca* strains immediately after initiation of CHV1-EP713 infection by transfection with infectious *in vitro* synthesized hypovirus CHV1-EP713 coding strand RNA transcripts. DI RNAs begin to appear during the second or third subculturing as a series of larger species in the range of ≈10-kb (not shown), followed by the formation of a smaller, ≈ 8-kb, stable form with the typical gel banding pattern shown in lane 1 of Fig. 1*A*. This DI RNA band was isolated, used as a template to generate cDNA, and amplified with three overlapping sets of

Author contributions: X.Z. and D.L.N. designed research, X.Z. performed research, X.Z. and D.L.N. analyzed data, and X.Z. and D.L.N. wrote the paper.

The authors declare no conflict of interest.

This article is a PNAS Direct Submission.

Freely available online through the PNAS open access option.

*To whom correspondence should be addressed at: Center for Biosystems Research, University of Maryland Biotechnology Institute, Shady Grove Campus, 9600 Gudelsky Drive, Rockville, MD 20850. E-mail: nuss@umbi.umd.edu.

This article contains supporting information online at www.pnas.org/cgi/content/full/0807225105/DCSupplemental.

MICROBIOLOGY

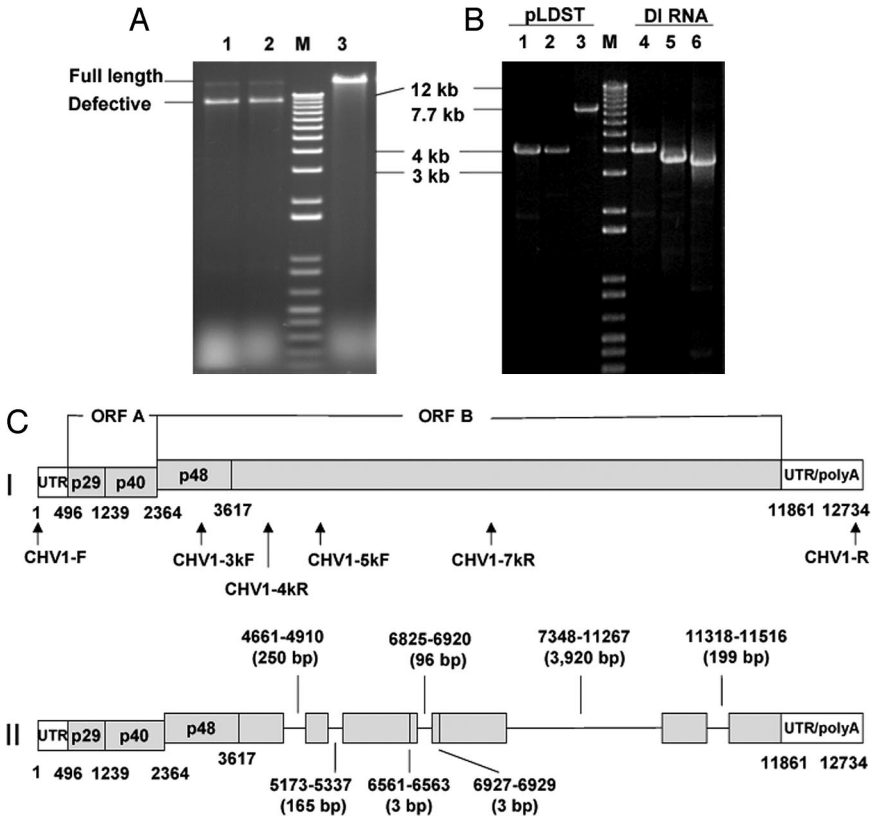

Fig. 1. Accumulation and characterization of hypovirus DI RNAs. (*A*) Agarose gel (1%) banding pattern of hypovirus dsRNAs isolated from hypovirus CHV1-EP713-infected wild-type *C. parasitica* strain EP155 (lane 1, 10 subcultures), dicer 1 gene deletion mutant strain Δ*dcl-1* strain (lane 2, 10 subcultures), and dicer-2 gene deletion mutant strain Δ*dcl-2* (lane 3, 17 subcultures). The migration positions of full-length CHV1-EP713 dsRNA and ≈8-kb DI RNA, formerly designated M-RNA (11), are shown in the left margin. The lane marked ''M'' contains the 1-kb ladder DNA size markers (Gibco). (*B*) PCR-amplified fragments from full-length CHV1-EP713 cDNA template plasmid pLDST (lanes 1–3) and from cDNA template generated from isolated ≈8 kb CHV1-EP713 DI RNA (lanes 4–6). Primer pairs CHV1-F/CHV1–4kR, CHV1–3kF/CHV1–7kR, and CHV1–5kF/CHV1-R were used, respectively, to amplify regions of the CHV1-EP713 genome corresponding to the 5′ terminus to 4 kb (lanes 1 and 4), 3 kb–7 kb (lanes 2 and 5), and 5 kb–12.7 kb (the 3′ terminus; lanes 3 and 6). The rational for primer selection was as follows. Primers spaced 1 kb along the viral genome RNA were tested for amplification of cDNA generated from isolated DI RNA. This exercise gave an estimate of the location of deleted regions. A subset of these primers (above) predicted to produce a set of overlapping PCR products that spanned the DI RNA was then selected. (*C*) Diagram of the structure of the major 8,098-nt-long CHV1-EP713-derived DI RNA shown in Fig. 1*A*, relative to the full-length parental viral RNA. The genetic organization of the parental hypovirus CHV1-EP713 RNA is shown at the top (I). The coding strand is 12,712 nucleotides, excluding the poly (A) tract, and contains two ORFs, ORFs A and B (35). ORF A encodes two polypeptides, p29 and p40, that are released from polyprotein p69 by an autocatalytic event mediated by the papain-like protease domain with p29 (36). An autocatalytic event also releases p48, a second papain-like protease, from the N terminus of the ORF B polyprotein, which contains RdRp and helicase domains. The positions of primer pairs used to amplify fragments shown in *B* are indicated below the full-length CHV1-EP713 RNA diagram. In (II), the positions of seven deletions found in the 8,098-nt DI RNA are indicated as lines, whereas the regions retained in the DI RNA are indicated by gray bars. The coordinates and size of each deletion is indicated above or below the DI RNA diagram.

primer pairs that spanned the CHV1-EP713 genome RNA map to give amplified fragments that extended from the 5′ terminus to 4 kb, from position 3 kb to 7 kb and from position 5 kb to 12.7 kb. (Fig. 1*B*). The tight banding patterns of the PCR products generated by each primer pair (Fig. 1*B*) indicated that the DI RNA population consisted of a predominant species. Differences in the migration positions for the fragments amplified from the full-length viral cDNA (pLDST) and from the DI RNA cDNA templates for the second and third primer pairs (compare lane 2 with lane 5 and lane 3 with lane 6) indicate deletions within the corresponding portions of the DI RNA.

Sequence analysis of the amplified DI RNA cDNA fragments revealed an 8,098-nt RNA containing a total of seven deletions relative to the full-length parental RNA (Fig. 1*C*). These included one major deletion of 3,920 bp (7348–11267), four small deletions of 250 bp (4661–4910), 165 bp (5173–5337), 96 bp (6825–6920), and 199 bp (11318–11516), and two very small deletions of 3 bp each (6561–6563; 6927–6929). The deletion break points are located in ORF B, beginning downstream of the p48 protein coding sequence and extending into the RNA-dependent RNA polymerase (RdRp) and helicase-coding domains [supporting information (SI) Fig. S1]. All deletions resulted in reading frame shifts and predicted early translational termination. The major 3,920-bp deletion in the defective RNA corresponded exactly to the region of low vsRNA abundance described previously (15). These findings support the prediction that decreased accumulation of regions of the viral genome that are deleted in the DI RNAs, and increased accumulation of the regions that are retained, contribute to an uneven vsRNA distribution in infected *C. parasitica* strains containing both DI RNAs and full-length viral genomes.

Hypovirus DI RNA Production Requires Host Dicer Gene *dcl-2*. DI RNAs have been shown to trigger the production of vsRNAs in tombusvirus-infected plants but to be poor targets for vsRNA-guided degradation (16). Havelda *et al.* (17) subsequently showed that the production of excess vsRNAs from the tombusvirus DI RNA saturated the binding of the silencing suppressor p19, whereas the escape from degradation resulted in a buildup in DI RNAs that could compete with helper virus RNA for replicase molecules.

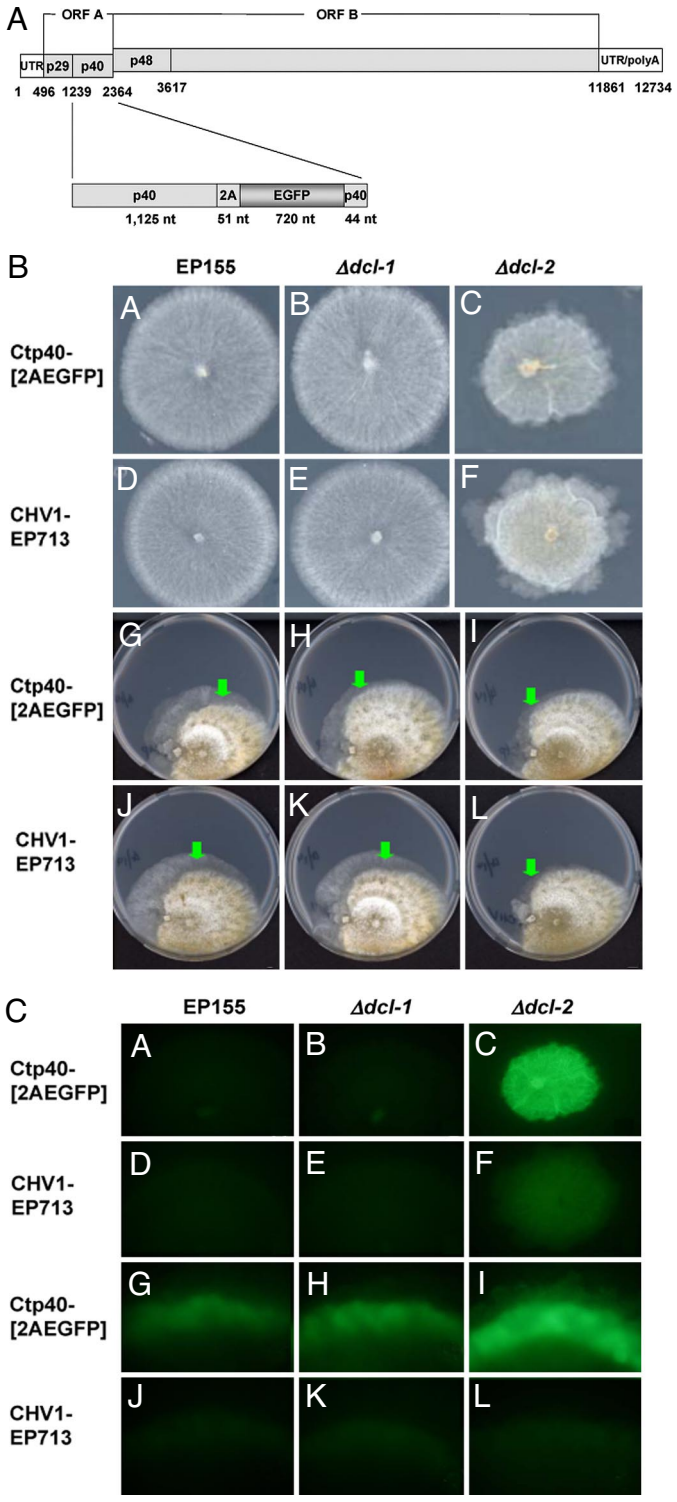

Fig. 2. Stability of nonviral sequences in recombinant hypovirus vector RNA. (*A*) Schematic representation of recombinant hypovirus EGFP vector Ctp40[2AEGFP]. The construction of Ctp40[2AEGFP] was previously described by Suzuki *et al.* (13) and involved the insertion of a cassette, consisting of the foot and mouth disease virus 2A protease domain fused to EGFP at the C terminus of p40, followed by a 44-nt duplication of the C-terminal portion of p40 to facilitated ribosomal reinitiation at the UAAUG junction between ORFs A and B. (*B*) Light micrographs of *C. parasitica* wild-type and dicer mutant strains infected with hypovirus CHV1-EP713 or recombinant hypovirus vector Ctp40[2AEGFP] and subcultured 10 times. CHV1-EP713- and Ctp40[2AEGFP]-infected Δ*dcl2* mutant strains (*C* and *F*, respectively) grow considerably slower than comparably infected wild-type strain EP155 (*A* and *D*) and the Δ*dcl-1* mutant strain (*B* and *E*) because of enhanced virus-mediated symptoms in the absence of the functional RNA silencing response (14). Consequently, the infected EP155 and Δ*dcl-1* strains were grown for 4 days and stored at 4°C, whereas the infected Δ*dcl-2* strains were grown for 7 days, and all colonies were photographed on day 7 after inoculation. Cytoplasmic transmission of CHV1-EP713 and recombinant vector Ctp40[2AEGFP] RNAs via anastomosis (fusion of hyphae) from infected Δ*dcl-2* strains to uninfected wild-type EP155 and Δ*dcl-1* and Δ*dcl-2* mutant strains is shown in *G–L*. For each plate, the CHV1-EP713- or Ctp40[2AEGFP]-infected Δ*dcl-2* donor strain is on the left and the virus-free recipient strain is on the right of the paired colonies. Virus-mediated conversion of the recipient strain as a result of anastomosis appears as a wedge of mycelia with characteristic virus-associated phenotypic alterations that initiate at the interface between the two colonies and extends along the periphery of the recipient colony. The green arrows indicate the region of the virus-converted recipient strain photographed under the fluorescence microscope. (*C*) Fluorescent micrographs of the colonies and anastomosis plates presented in *B* using conditions described in *Materials and Methods*. The CHV1-EP713–infected Δ*dcl-2* colony (*F*) exhibited a higher level of background fluorescence background because of a compact growth phenotype. For *G–L*, the regions indicated by the green arrows in *B* were rotated to the horizontal orientation for uniformity.

The influence of RNA silencing on hypovirus DI RNA production and accumulation was examined by transfecting *C. parasitica* wild-type and dicer gene disruption mutant strains Δ*dcl-1* and Δ*dcl-2* with infectious, *in vitro* synthesized hypovirus CHV1-EP713 coding strand RNA transcripts. A progression of DI RNA production, similar to that seen in wild-type infected *C. parasitica*, was observed for dicer 1 disruption strain Δ*dcl-1* transfected with CHV1-EP713 RNA, resulting in an identical banding pattern and predominance of the DI RNA relative to the full-length viral RNA (Fig. 1*A*, lanes 2 and 3). In sharp contrast, no DI RNA was produced in strains disrupted for the dicer 2 gene, Δ*dcl-2*, even after prolonged infection (e.g., more than 17 subcultures; Fig. 1*A*, lane 3).

Not only did DI RNA fail to form in Δ*dcl-2* strains, but also DI RNAs present in wild-type strain EP155 were lost when CHV1-EP713 RNA was transmitted to the Δ*dcl-2* strain by anastomosis (fusion of hyphae) (data not shown). However, the DI RNAs reappeared after several subcultures following anastomosis-mediated transfer of hypovirus RNA from the Δ*dcl-2* strain back to the wild-type strain. DI RNAs also formed readily following anastomosis-mediated transfer of CHV1-EP713 RNA to the Δ*dcl-2* mutant strain that had been complemented (described in 14) with a genomic clone of the *dcl-2* gene (data not shown). Based on the foregoing observations, we conclude that *dcl-2* is required for hypovirus DI RNA production.

Dicer *dcl-2* Is Required for Instability of Nonviral Nucleotide Sequences in Recombinant Viral RNA. The requirement of *dcl-2* for hypovirus DI RNA production suggests that DCL-2 plays a key role in hypovirus RNA recombination. We previously reported that nonviral gene sequences inserted into replication competent recombinant CHV1-EP713 were subject to recombination and deleted within one to two subcultures after transfection (13). Thus, it was of interest to test the stability of hypovirus recombinant vectors in the dicer deletion mutant strains.

The potential role of *dcl-2* in RNA virus vector instability was tested by transfecting wild-type and dicer deletion mutant strains with the vector construct Ctp40[2AEGFP] (Fig. 2*A*), which contains the enhanced green fluorescent protein (EGFP) coding domain proceeded by the foot and mouth disease virus (FMDV) 2A protease domain inserted into the p40 coding region just upstream of the ORF A–ORF B junction.

Wild-type EP155 and Δ*dcl-1* mutant strains transfected with Ctp40[2AEGFP] coding strand RNA began producing deleted RNA at the second subculture (2 weeks after the original colonies were recovered from the regeneration plates) and

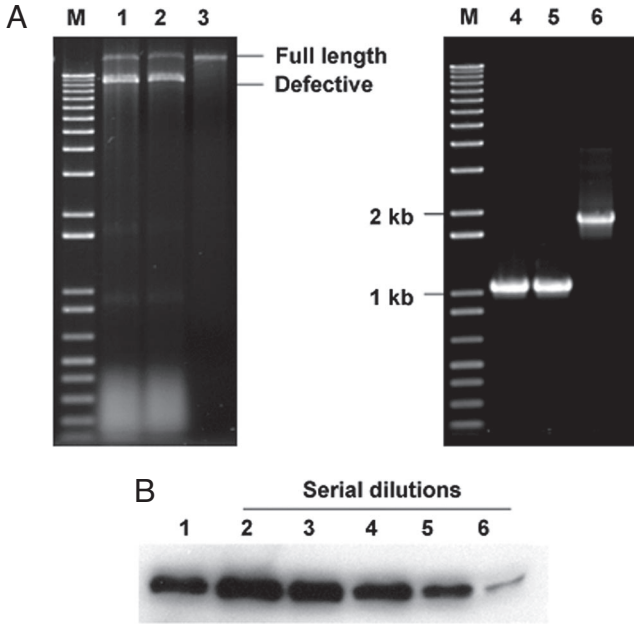

Fig. 3. Analysis of recombinant hypvoirus Ctp40[2AEGFP] stability and directed EGFP expression levels after 10 subcultures. (*A Left*) Agarose (1%) gel analysis of dsRNAs recovered from Ctp40[2AEGFP]-infected wild-type strain EP155 (lane 1), dicer-1 mutant strain Δ*dcl-1* (lane 2), and dicer-2 mutant strain Δ*dcl-2* (lane 3). The lane marked ''M'' contains 1-kb DNA size markers. The migration positions of full-length Ctp40[2AEGFP] RNA and DI RNAs are indicated on the right. (*Right*) RT-PCR analysis of the Ctp40[2AEGFP] RNA recovered from wild-type strain EP155 (lane 4) and mutant strains Δ*dcl-1* (lane 5) and Δ*dcl-2* (lane 6) for the presence of the 2A/EGFP nonviral sequences. The region containing the 2A/EGFP sequences in the original recombinant Ctp40[2AEGFP] RNA used to initiate infections was amplified with primer pairs CHV1–2kF and CHV1–3kR corresponding to the CHV1-EP713 map positions 2 kb and 3 kb that flank the insertion site. (*B*) Endpoint dilution immunoblot analysis of EGFP expression directed by vector Ctp40[2AEGFP] in strain Δ*dcl-2* relative to that produced in the EGFP-transformed strain EP155/EGFP-Bn, similar to that reported by Parsley *et al.* (18). Lane 1, 1 μg of total protein from EP155/EGFP-Bn; lanes 2–6, 1 μg, 400 ng, 200 ng, 100 ng, and 50 ng of protein, respectively, from the Δ*dcl-2*/Ctp40[2AEGFP] strain (1-, 2.5-, 5-, 10-, and 20-fold dilution, respectively). The EGFP expressed in the transgenic EP155/EGFP-Bn strain and the Ctp40[2AEGFP]-infected strain migrated with the same mobility and consistent with a size of 27 kDa.

produced weak fluorescence at the first transfer, followed by a rapid reduction in fluorescence signal to undetectable levels. In contrast, the Δ*dcl-2* strain transfected with Ctp40[2AEGFP] maintained a single dsRNA band corresponding to full-length Ctp40[2AEGFP] RNA (Fig. 3*A*, lane 3) and exhibited strong fluorescence for over 10 passages (Fig. 2*C*). PCR analysis of the insert with primers spanning the nonviral sequences confirmed that the ≈800-nt foreign insert was completely removed from viral genome in wild-type EP155 and Δ*dcl-1* mutant strains but was retained intact in the Δ*dcl-2* mutant strain (Fig. 3*A*, lane 6). Western blot analysis of a serial dilution of protein extracted from the Ctp40[2AEGFP]-infected Δ*dcl-2* strain (Δ*dcl-2*/Ctp40[2AEGFP]) (Fig. 3*B*) showed that the EGFP protein was expressed from the viral vector in Δ*dcl-2* at passage 10 at levels between 5- and 10-fold greater than those produced from a nuclear copy of the EGFP gene in a transgenic wild-type EP155 strain (18). Moreover, the EGFP protein expressed from the Ctp40[2AEGFP] virus in Δ*dcl-2* migrated with similar mobility as the transgene-expressed EGFP (Fig. 3*B*), suggesting that the protease 2A efficiently cleaved EGFP from the p40 fusion protein.

The EGFP-expressing Ctp40[2AEGFP] RNA-infected Δ*dcl-2* strain was paired (anastomosed) with uninfected wild-type EP155, Δ*dcl-1*, and Δ*dcl-2* strains to examine the transmission and subsequent stability of the viral vector. Ctp40[2AEGFP] RNA was successfully transmitted to each of the uninfected strains and young recipient mycelia near the contact area showed strong EGFP fluorescence (Fig. 2 *B* and *C*). The EGFP-expressing mycelia from each plate were transferred to new plates for serial subculture. Similar to in the transfection experiment, EGFP fluorescence disappeared after two transfers of the EP155/ Ctp40[2AEGFP] and Δ*dcl-1*/Ctp40[2AEGFP] strains but was completely stable in the Δ*dcl-2*/Ctp40[2AEGFP] strain through multiple transfers (data not shown). These combined results demonstrate that nonvirus vector sequences are stable for prolonged periods in strains lacking *dcl-2*, but are deleted from the viral vector within one or two subcultures in strains containing *dcl-2*.

Discussion

The conventional view holds that DI RNAs are generated from the parental viral RNA genome as a result of replicase-mediated recombination deletion events and are then further selected for the presence of *cis* elements that promote their replication by the parental helper virus (2). Recent reports that DI RNAs are effective inducers but poor targets of virus-induced RNA silencing (16, 17) have led to the proposal that the host RNA-silencing antiviral defense response also influences the selection and accumulation of DI RNAs relative to the parental helper virus by eliminating DI RNA sequences that are vulnerable RNA-silencing targets (3). We report a more fundamental role of RNA silencing in DI RNA biogenesis by showing that the production of DI RNAs from a positive sense RNA hypovirus requires a specific host dicer gene, *dcl-2*, previously shown to be induced by virus infection and to be solely responsible for vsRNA biogenesis (15).

The role of *dcl-2* in hypovirus RNA recombination also extends to the deletion of nonviral nucleotide sequences from recombinant hypovirus RNA vectors (Figs. 2 and 3). Although targeted RNA silencing of nonviral sequences has been reported to influence (increase) the stability of the foreign gene insert in one RNA virus vector (19) but not in another (20), our results demonstrate a requirement for a specific component of the RNA-silencing pathway for the elimination of nonviral sequences from viral vector RNA.

Hypovirus coding strand RNA is infectious by transfection of fungal spheroplasts, a hallmark of positive sense RNA viruses (21). Comparative sequence analysis has suggested a common ancestry between hypoviruses and the single-strand, positive sense plant-infecting potyviruses (22), members of the picornavirus supergroup (23). A high degree of sequence conservation was observed for the RNA-dependent RNA polymerase (RdRp) and helicase domains of the two virus groups. Hypovirus RdRp activity is associated with membrane vesicles isolated from infected mycelia (24), and the RdRp reaction products consist primarily of coding strand RNA transcripts and a smaller amount of full-length dsRNA that corresponds to replicative intermediate or replicative form structures. The structural properties of the hypovirus DI RNAs also share common features with DI RNAs from other RNA viruses. These RNAs are unable to replicate autonomously and retain the 5′ and 3′ terminal domains and noncontiguous portions of the central region of the parental virus RNA (Fig. 2 and refs. 11, 12). The similarities in the basic elements of replication and DI RNA structure for hypoviruses and other major positive sense RNA virus taxonomic groups suggest a potentially broad role for dicer activity, and perhaps other RNA-silencing pathway components, in RNA virus recombination, DI RNA formation, and nonviral vector sequence instability. This prediction is most likely to hold for viruses replicating in plants where RNA silencing clearly functions as an antiviral defense mechanism (25). It will be of particular interest to examine whether the RNA-silencing path-

way also influences the frequent production of DI RNAs observed in RNA virus-infected animal cells (25), an environment in which the antiviral interferon response predominates.

The observation that full-length viral RNA was efficiently transmitted from a wild-type donor strain to the Δ*dcl-2* recipient strain by anastomosis, whereas the more abundant defective RNAs were lost in the transfer, raises some interesting points. Either there exists a specific restriction to the transfer of defective RNAs during anastomosis (an unlikely possibility) or the accumulation of defective RNAs is a dynamic process in the wild-type strain, and the defective RNA population is not replenished as the defective RNAs turnover after transfer to the Δ*dcl-2* strain. In the latter scenario, the mechanism of defective RNA turnover would have to be independent of RNA silencing, because this pathway is compromised in the Δ*dcl-2* strain. An alternative explanation, which runs counter to the currently accepted view, is that replication of parental viral RNA is favored over DI RNA replication in the absence of a functional RNA-silencing pathway. The observed dependence of hypovirus DI RNA production on *dcl-2* provides new opportunities to examine the dynamics of DI RNA biogenesis, replication, and degradation.

The classical copy-choice mode for DI RNA formation predicts that the viral RdRp switches templates during RNA replication (26, 27). This is thought to involve pausing and dissociation of the RdRp, along with the nascent RNA strand, from the template and reinitiation at a new position on the same or a different template. Within the framework of this model, DCL-2–dependent cleavage of the full-length CHV1-EP713 RNA at structured regions would liberate 5′ and 3′ fragments that could serve as substrates for the copy-choice template-switching mechanism. A similar type of model was recently proposed for the contribution of an endonuclease, Ngl2p, to recombination of tomato bushy stunt virus RNA in the yeast *Saccharomyces cerevisiae* (28), an organism that does not have an active RNA-silencing pathway (29). Irrespective of the precise role of DCL-2 in defective RNA production, the apparent absence of hypovirus defective RNAs in the infected Δ*dcl-2* strain indicates that errors by the viral RdRp likely are necessary, but insufficient, to produce defective RNA accumulation.

Although it is reasonable to predict that DCL-2–dependent production of fragments from hypovirus vector RNA will promote RNA recombination, the mechanism underling the rapid (and apparently preferential) targeting of the nonviral vector sequence for elimination is more difficult to envision. Although a mechanistic understanding requires evaluation of the stability of a range of foreign inserts that differ in size, sequence, and position, clearly nonviral vector sequences in vector Ctp40[2AEGFP] (Fig. 3) and vector p29Δ25–243EGFP2A (13; data not shown) that are rapidly deleted in wild-type *C. parasitica* strains remain stable for prolonged periods of infection in Δ*dcl-2* mutant strains. In this regard, it may be possible to increase the stability of nonviral sequences in RNA virus vectors by incorporating strong suppressors of RNA silencing or otherwise targeting RNA-silencing pathway components.

DCL-2 may function independently of other components of the RNA-silencing pathway to promote defective RNA production and the elimination of nonviral vector sequences. Studies of interactions between DCL-2 and predicted structured regions of hypovirus RNA and the nature of DCl-2 cleavage products are currently in progress. Contributions of downstream components of the RNA-silencing pathway, such as active vsRNA guide RNA–containing RISC complexes (30) and vsRNA-primed host RdRp activity (31), also are possible. The potential role of additional RNA-silencing pathway components in hypovirus defective RNA production and nonviral vector sequence instability is currently under investigation.

Materials and Methods

Fungal Strains and Growth Conditions. *C. parasitica* strain EP155 and dicer gene mutant strains Δ*dcl-1* and Δ*dcl-2* (14) were maintained on potato-dextrose agar (PDA; Difco) at 22°C to 24°C as described previously (32). Strains were cultured on cellophane membrane overlaid on the PDA medium for 7 days for RNA and protein isolation. Strains were transferred to new plates every 7 days (one passage).

Nucleic Acid Purification, Reverse-Transcription PCR, Protein Preparation, and Western Blot Analysis. Total RNA was prepared from fungal cultures as described previously (33). Purified total RNA was separated on 1% agarose gels. The M-size defective RNA was recovered with the QIAquick gel extraction kit (Qiagen). Then ≈100 ng of purified defective RNA was reverse-transcribed with SuperScript III reverse-transcriptase (Invitrogen) according to the manufacturer's instructions. The primer used for reverse-transcription (RT) of defective RNA was CHV1-R: 5′ GGATCC gcggccgc CTTTGTTGTTCTCTTCCC 3′ (with lower-case letters indicating a NotI endonuclease site for cloning purposes), a reverse primer located at the 3′ end of hypovirus CHV1-EP713 genome adjacent to the poly(A) tail. This RT reaction synthesized a complementary strand of the viral plus strand. The RT product was then PCR-amplified by three pairs of primers: CHV1-F/CHV1–4kR, CHV1–3kF/CHV1–7kR, and CHV1–5kF/CHV1-R. The primer sequences used in this study are listed in Table S1. These primer sets amplified three overlapping cDNA sequences corresponding to coordinates 5′terminus to 4 kb, 3 kb–7 kb, and 5 kb–12.7 kb (i.e., 3′ terminus) of the viral genome. The amplified PCR fragments were purified and sequenced with the primers listed in Table S1. For the *egfp/2A* insert stability assay, total RNA was extracted and reverse-transcribed with reverse primer CHV1–3kR, followed by PCR amplification with CHV1–2kF and CHV1–3kR. These two primers amplify the region corresponding to coordinates 2 kb–3 kb of the viral genome. Protein extraction and Western blot analysis were performed as described previously (34). The GFP rabbit polyclonal antibody used for Western blot analysis was purchased from Santa Cruz Biotechnology.

EGFP Viral Vector Transfection and Visualization of EGFP Fluorescence. The hypovirus construct Ctp40[2AEGFP] with insertions of the EGFP gene (*egfp*) and the FMDV 2A protease gene at the 3′ end of p40 was constructed previously (13). The generation of *in vitro* transcripts and the transfection into EP155, Δ*dcl-1*, and Δ*dcl-2* spheroplasts were as described by Suzuki *et al.* (13). Transfected fungal strains were cultured on cellophane membranes overlaying PDA plates. Infected strains EP155 and Δ*dcl-1* were placed at 4°C after 4 days of growth, whereas the slower-growing infected Δ*dcl-2* strains were cultured for 7 days. Fluorescence was observed with a fluorescence stereomicroscope (model MVX10; Olympus). Fluorescence micrographs were obtained with an Olympus model DP70 microscope digital camera and DP Manager version 2.2.1.195 software.

ACKNOWLEDGMENTS. This study was supported in part by U.S. Public Health Service Grant GM55981 (to D.L.N.).

1. Cheng C-P, Nagy PD (2003) Mechanism of RNA recombination in Carmo- and Tombusviruses: evidence for template switching by the RNA-dependent RNA polymerase *in vitro*. *J Virol* 77:12033–12047.
2. Roux L, Simon AE, Holland JJ (1991) Effects of defective interfering viruses on virus replication and pathogenesis. *Adv Virus Res* 40:181–211.
3. Simon AE, Roossinck MJ, Havelda Z (2004) Plant virus satellite and defective interfering RNAs: new paradigms for a new century. *Annu Rev Phytopathol* 42:415–437.
4. Holland JJ (1990) in *Virology*, eds Fields BN *et al.* (Raven, New York), pp 156–165.
5. Huang AS, Baltimore D (1970) Defective viral particles and viral disease processes. *J Mol Biol* 47:275–291.
6. de Haan CA, Haijema BJ, Boss D, Heuts FW, Rottier PJ (2005) Coronaviruses as vectors: stability of foreign gene expression. *J Virol* 79:12742–12751.
7. Scholthof HB, Scholthof K-BG, Jackson AO (1996) Plant virus gene vectors for transient expression of foreign proteins in plants. *Annu Rev Phytopathol* 34:299–323.
8. Paar M, *et al.* (2007) Effects of viral strain, transgene position, and target cell type on replication kinetics, genome stability, and transgene expression of replication-competent Murine Leukemia Virus–based vectors. *J Virol* 81:6973–6983.
9. van den Born E, Posthuma CC, Knoops K, Snijder EJ (2007) An infectious recombinant equine arteritis virus expressing green fluorescent protein from its replicase gene. *J Gen Virol* 88:1196–1205.

10. Lee SG, Kim DY, Hyun BH, Bae YS (2002) Novel design architecture for genetic stability of recombinant poliovirus: the manipulation of G/C contents and their distribution patterns increases the genetic stability of inserts in a poliovirus-based RPS-Vax vector system. *J Virol* 76:1649–1662.
11. Shapira R, Choi GH, Hillman BI, Nuss DL (1991) The contribution of defective RNAs to the complexity of viral-encoded double-stranded RNA populations present in hypovirulent strains of the chestnut blight fungus *Cryphonectria parasitica. EMBO J* 10:741–746.
12. Hillman BI, Foglia R, Yuan W (2000) Satellite and defective RNA of *Cryphonectria* hypovirus-3 grand haven 2, a virus species in the family *Hypoviridae* with a single open reading frame. *Virology* 276:181–189.
13. Suzuki N, Geletka LM, Nuss DL (2000) Essential and dispensible virus-encoded replication elements revealed by efforts to develop hypoviruses as gene expression vectors. *J Virol* 74:7568–7577.
14. Segers GC, Zhang X, Deng F, Sun Q, Nuss DL (2007) Evidence that RNA silencing functions as an antiviral defense mechanism in fungi. *Proc Natl Acad Sci USA* 104:12902–12906.
15. Zhang X, Segers GC, Sun Q, Deng F, Nuss DL (2008) Characterization of hypovirus-derived small RNAs generated in the chestnut blight fungus by an inducible DCL-2–dependent pathway. *J Virol* 82:2613–2619.
16. Szittya G, Molnar A, Silhavy D, Hornyik C, Burgyan J (2002) Short defective interfering RNAs of Tombusviruses are not targeted but trigger post-transcriptional gene silencing against their helper virus. *Plant Cell* 14:359–372.
17. Havelda Z, Hornyik C, Valoczi A, Burgyan J (2005) Defective interfering RNA hinders the activity of a Tombusvirus-encoded posttranscriptional gene silencing suppressor. *J Virol* 79:450–457.
18. Parsley TB, Chen B, Geletka LM, Nuss DL (2002) Differential modulation of cellular signaling pathways by mild and severe hypovirus strains. *Eukaryotic Cell* 1:401–413.
19. Zhong X, Hou H, Qiu W (2005) Integrity of nonviral fragments in recombinant Tomato bushy stunt virus and defective interfering RNA is influenced by silencing and the type of insert. *Mol Plant-Microbe Interact* 18:800–807.
20. Barajas D, Tenllado F, Diaz-Ruiz JR (2006) Characterization of the recombinant forms arising from a Potato virus *X* chimeric virus infection under RNA silencing pressure. *Mol Plant-Microbe Interact* 19:904–913.
21. Chen B, Choi GH, Nuss DL (1994) Attenuation of fungal virulence by synthetic infectious hypovirus transcripts. *Science* 264:1762–1764.
22. Koonin EV, Choi GH, Nuss DL, Shapira R, Carrington JC (1991) Evidence for common ancestry of a chestnut blight hypovirulence–associated double-stranded RNA and a group of positive-strand RNA plant viruses. *Proc Natl Acad Sci USA* 88:10647–10651.
23. Ryan MD, Flint M (1997) Virus-encoded proteinases of the picornavirus super-group. *J Gen Virol* 78:699–723.
24. Fahima T, Kazmierczak P, Hansen DR, Pfeiffer P, Van Alfen NK (1993) Membrane-associated replication of an unencapsidated double-stranded RNA of the fungus, *Cryphonectria parasitica. Virology* 195:81–89.
25. Ding SW, Voinnet O (2007) Antiviral immunity directed by small RNAs. *Cell* 130:413–426.
26. Lazzarini RA, Keene JD, Schubert M (1981) The origins of defective interfering particles of the negative strand RNA viruses. *Cell* 26:145–154.
27. Kirkegaard K, Baltimore D (1986) The mechanism of RNA recombination in poliovirus. *Cell* 47:433–443.
28. Cheng CP, Serviene E, Nagy PD (2006) Suppression of viral RNA recombination by a host exoribonuclease. *J Virol* 80:2631–2640.
29. Nakayashiki H, Kadotani N, Mayama S (2006) Evolution and diversity of RNA silencing proteins in fungi. *J Mol Evol* 63:127–135.
30. Tomari Y, Zamore PD (2005) Perspective: machines for RNAi. *Genes Dev* 19:517–529.
31. Chapman EJ, Carrington JC (2007) Specialization and evolution of endogenous small RNA pathways. *Nat Rev Genet* 8:884–896.
32. Hillman BI, Shapira R, Nuss DL (1991) Hypovirulence-associated suppression of host functions in *Cryphonectria parasitica* can be partially relieved by high light intensity. *Phytopathology* 80:950–956.
33. Suzuki N, Nuss DL (2002) Contribution of protein p40 to hypovirus-mediated modulation of fungal host phenotype and viral RNA accumulation. *J Virol* 76:7747–7759.
34. Deng F, Nuss DL (2008) Hypovirus papain-like protease p48 is required for initiation but not for maintenance of virus RNA propagation in the chestnut blight fungus *Cryphonectria parasitica. J Virol* 82:6369–6378.
35. Shapira R, Choi GH, Nuss DL (1991) Virus-like genetic organization and expression for a double-stranded RNA genetic element associated with biological control of chestnut blight. *EMBO J* 10:731–739.
36. Choi GH, Shapira R, Nuss DL (1991) Cotranslational autoproteolysis involved in gene expression from a double-stranded RNA genetic element associated with hypovirulence of chestnut blight. *Proc Natl Acad Sci USA* 88:1167–1171.